

Published in final edited form as:

*Biochim Biophys Acta*. 2014 June ; 1843(6): 1054–1062. doi:10.1016/j.bbamcr.2014.02.010.

## mTOR-INDEPENDENT INDUCTION OF AUTOPHAGY IN TRABECULAR MESHWORK CELLS SUBJECTED TO BIAXIAL STRETCH

Kristine M. Porter, Nallathambi Jeyabalan, and Paloma B. Liton\*

Duke University, Department of Ophthalmology, Durham, NC, USA

### Abstract

The trabecular meshwork (TM) is part of a complex tissue that controls the exit of aqueous humor from the anterior chamber of the eye, and therefore helps maintaining intraocular pressure (IOP). Because of variations in IOP with changing pressure gradients and fluid movement, the TM and its contained cells undergo morphological deformations, resulting in distention and stretching. It is therefore essential for TM cells to continuously detect and respond to these mechanical forces and adapt their physiology to maintain proper cellular function and protect against mechanical injury. Here we demonstrate the activation of autophagy, a pro-survival pathway responsible for the degradation of long-lived proteins and organelles, in TM cells when subjected to biaxial static stretch (20 % elongation), as well as in high-pressure perfused eyes (30 mm Hg). Morphological and biochemical markers for autophagy found in the stretched cells include elevated LC3-II levels, increased autophagic flux, and the presence of autophagic figures in electron micrographs. Furthermore, our results indicate that the stretch-induced autophagy in TM cells occurs in an MTOR- and BAG3-independent manner. We hypothesize that activation of autophagy is part of the physiological response that allows TM cells to cope and adapt to mechanical forces.

### Keywords

autophagy; glaucoma; mechanical stress; trabecular meshwork; MTOR pathway; chaperon-assisted autophagy

### INTRODUCTION

The trabecular meshwork (TM) is part of a complex tissue that controls the exit of aqueous humor (AH) from the anterior chamber of the eye. Aqueous humor is continuously produced by the ciliary body and enters the anterior chamber through the pupil, draining passively out of the eye in a pressure gradient manner *via* first the TM and then through the Schlemm's

© 2014 Elsevier B.V. All rights reserved

\*Corresponding Author: Paloma B. Liton Duke University Eye Center AERI Bldg, Office 4004 Erwin Rd. Box 3802 Durham, NC 27713 Phone: (919) 681 4085 paloma.liton@dm.duke.edu.

**Publisher's Disclaimer:** This is a PDF file of an unedited manuscript that has been accepted for publication. As a service to our customers we are providing this early version of the manuscript. The manuscript will undergo copyediting, typesetting, and review of the resulting proof before it is published in its final citable form. Please note that during the production process errors may be discovered which could affect the content, and all legal disclaimers that apply to the journal pertain.

canal. The rate of AH drainage must be equal to AH production. Resistance to AH outflow causes elevated intraocular pressure (IOP), and with that the risk of developing glaucoma, the second leading cause of irreversible permanent blindness worldwide [1].

Because of variations in IOP with changing pressure gradients and fluid movement, the TM constantly undergoes morphological deformations. Increased IOP results in distention and stretching of the TM and its contained cells, while decreased IOP leads to relaxation of the tissue [2,3]. The TM is subjected to additional sources of strain originated by ciliary muscle contraction, with mechanical forces stretching it from Schwalbe's line to the scleral spur, and inwards towards the Schlemm's canal lumen [3]. Transient changes in IOP are also experienced during blinking or squeezing of the lid, manual eye rubbing, Valsava manouvers, and other activities [4]. It is therefore essential for TM cells to continuously detect and respond to these mechanical forces, and adapt their physiology in order to maintain proper cellular function and protect against mechanical injury. In this sense, several groups have already shown that mechanical stress can trigger a broad range of responses in TM cells, including changes in cytoskeleton, induction of gene expression, and activation of regulatory pathways [5–19]. However, little is known about the strategies that are used by TM cells to respond to this stress, so they can adapt and survive.

Autophagy is a degradative process whereby cytosolic components such as proteins and organelles are captured and broken down *via* the lysosomal pathway. Although it was long believed that autophagy was a cell response to starvation, research has shown that autophagic degradation fulfills a number of physiological roles including promoting cell survival and adaptation, not only to metabolic but other cytotoxic stresses [20]. There are at least three types of autophagy, based on the different pathways by which cargo material is delivered to the lysosomes for degradation. Among those, macroautophagy, hereafter referred to as autophagy, is the most widely studied and best characterized process. This particular type of autophagy is characterized by the formation of a cytosolic double-membrane vesicle, the autophagosome, which engulfs the material to be degraded. Autophagosomes then fuse with lysosomes to form autolysosomes, in which the cytoplasmic cargos are degraded by resident hydrolases. The resulting degradation products are then transported back into the cytosol through the activity of membrane permeases for reuse. All these steps are highly regulated by a number of evolutionary conserved autophagy related genes (ATG genes) and ubiquitin-like conjugation systems [21].

A key event required for activation of autophagy is the lipidation of the autophagosome marker LC3-I to LC3-II. LC3 is synthesized as a precursor form that is cleaved by the protease ATG4B, resulting in the cytosolic isoform LC3-I. Upon induction of autophagy, LC3-I is conjugated to phosphatidylethanolamine to form LC3-II. LC3-II is incorporated to the nascent and elongating autophagosome membrane and remains on the autophagosome until fusion with the lysosomes. In the autolysosomes LC3-II is then either degraded or delipidated by ATG4 and recycled [22–24]. The kinase MTOR is a critical regulator of autophagy induction, with activated MTOR suppressing autophagy [25,26].

In this study we show that autophagy is activated in TM cells in an MTOR-independent manner in response to static biaxial stretch and in high-pressure perfused eyes. We

hypothesize that activation of autophagy is part of the physiological response to maintain TM cellular homeostasis and adaptation to mechanical forces.

## MATERIALS AND METHODS

### Reagents

3-Methyladenine (3-MA, Sigma-Aldrich, M9281), bafilomycin A1 (Sigma-Aldrich, B1793), cycloheximide (Chx, Sigma-Aldrich, C7698), chloroquine (CQ, Sigma-Aldrich, C6628), and rapamycin (Calbiochem, 553210).

### Cell Cultures

Primary cultures of porcine and human TM cells were prepared and maintained as previously described [27]. Briefly, the TM was dissected and digested with 2 mg/mL of collagenase for 1 hour at 37 °C. The digested tissue was placed in gelatin-coated 35 mm dishes and cultivated in low glucose Dulbecco's Modified Eagle Medium (DMEM) with L-glutamine and 110 mg/L sodium pyruvate, supplemented with 10% fetal bovine serum (FBS), 100 mM non-essential amino acids, 100 units/ml penicillin, 100 mg/ml streptomycin sulfate and 0.25 mg/ml amphotericin B; all the reagents were obtained from Invitrogen (Carlsbad, CA). Cells were maintained and propagated until passage three at 37 °C in a humidified air with 5% CO<sub>2</sub> incubator. Cell lines were subcultivated 1:2 when confluent. Primary cultures of porcine TM cells were prepared from porcine cadaver eyes obtained from a local abattoir (City Packing CO, Burlington, NC) less than five hours post-mortem. Primary cultures of human TM cells were prepared from residual cornea rims after surgical corneal transplantation at Duke University Eye Center. The protocols involving the use of human tissue were consistent with the tenets of the Declaration of Helsinki. Cells at passage four or five were used. Cultures labeled with the same number indicate same cell line. The transformed TM human cell line (NTM) were kindly provided by Alcon Research [28].

### Mechanical Stress Application

Mechanical stress was applied using the computer-controlled, vacuum-operated FX-3000 Flexercell Strain Unit (Flexcell, Hillsborough, NC). For this, cells were plated on type I collagen-coated flexible silicone bottom plates (Flexcell, Hillsborough, NC). Once confluency was reached, cells were subjected to static stretch (20% elongation) for the indicated times in each experiment. Control cells were cultured under the same conditions, but no mechanical force was applied. When indicated, chloroquine (CQ, 30 nM), Bafilomycin A1 (BafA1, 100 nM), 3-methyladenine (3-MA, 10 mM), or cyclohexamide (Chx, 25 µM) were added to the culture media one hour prior to stretching.

### Obtention of Whole Cell Protein Lysates

Cells were washed twice in PBS and lysated in 20 mM HEPES, 2 mM EGTA, 5 mM EDTA, and 0.5% NP-40 containing protease inhibitor cocktail (Thermo Scientific, 1858566) and phosphatase inhibitor cocktail (Thermo Scientific, 78420). After sonication for one minute on ice, the lysates were clarified by centrifugation. Protein concentration was determined with a protein assay kit (Micro BCA, Thermo Scientific, 23235).

### Western Blot Analysis

Protein samples (10  $\mu$ g) were separated by 10% polyacrylamide SDS-PAGE gels (15% polyacrylamide for LC3 detection, 7% polyacrylamide for filamin detection) and transferred to PVDF membranes (Bio-Rad, 162-0177). The membranes were blocked with 5% nonfat dry milk and incubated overnight with the specific primary antibodies. The bands were detected by incubation with a secondary antibody conjugated to horseradish peroxidase and chemiluminescence substrate (ECL Plus, GE Healthcare, RPN2132). Antibodies used are listed in Table 1.

### Electron microscopy

Cells were washed twice in PBS and fixed in 2.5% glutaraldehyde in 0.1M cacodylate buffer (pH 7.2). Fixed cells were then detached by gentle scraping, pelleted, post-fixed in 1% osmium tetroxide in 0.1M cacodylate buffer, and processed for transmission electron microscopy in the Morphology Facility at Duke Eye center. Perfused eyes were opened at the equator and the anterior segment was fixed in 2.5% glutaraldehyde and 2% formaldehyde. Thin sections (65 nm) were examined in a JEM-1200EX electron microscopy.

### Monitoring autophagy dynamics using Adtflc3

Trabecular meshwork cells grown on Flexcell plates were transduced with 10 pfu/ cell of the replication-deficient adenovirus containing LC3 fused to GFP and RFP (Adtflc3) as previously described [29]. At 2 dpi, cells were subjected to static mechanical stress (20% elongation, 1 hour). Cells were then washed in PBS and fixed for ten minutes at room temperature in 4% paraformaldehyde. Images were taken by confocal microscopy in a Zeiss LSM 510 upright microscope using a 63 $\times$ /1.0 dipping objective. Images from five different fields were taken in each individual experiment. Red and yellow puncta were counted in a masked manner both manually, by two independent investigators, and automatically using the Green and Red Puncta Co-localization Image J Plugin (D. J. Swiowski modified by R. K. Dagda, and coapproved as an image tool for autophagic flux by Charleen T. Chu). A total of two cells per field were counted (ten cells per experiment). Experiments were repeated three times using different cell lines (total cells counted per condition = 30). To facilitate manual counting the Find Edges process in Image J was applied to the images.

### siRNA Transfection

NTM cells grown on Flexcell plates were transfected with either 100 pmol siRNA against BAG3 (siBAG3) or 100 pmol non-targeting siRNA (siNC) using Lipofectamin RNAiMax Reagent, following the manufacturer's instructions. Cells were kept overnight in Opti-MEM medium and then switched to 10% DMEM. Cells were subjected to mechanical stress at day 2 post-transfection.

### Whole Eye Perfused Organ Culture

Enucleated porcine eyes were obtained from a local abattoir (City Packing CO, Burlington, NC) less than two hours post-mortem and maintained at 4  $^{\circ}$ C until use. Eyes were cleaned of extraocular tissue and a 23-gauge needle was inserted intracamerally through the cornea and

placed in the posterior chamber. One eye of each pair was perfused at a constant normal pressure of 8 mmHg (equivalent to 15 mmHg *in vivo*), while the fellow eye was perfused at high pressure (40 mmHg) for 1 hour at 37 °C in a humidified air with 5% CO<sub>2</sub> incubator. Dulbecco's phosphate-buffered saline (DPBS; pH 7.4) supplemented with 5.5 mM D-glucose was used as perfusion media. Immediately after perfusion, eyes were opened at the equator and the anterior segment fixed in 2.5% glutaraldehyde and 2% formaldehyde for EM studies, or the TM dissected and quick-froze for WB analysis.

### Statistical analysis

All experimental procedures were repeated at least three times in independent experiments using different cell lines and pair of eyes. Data are represented as mean  $\pm$  SD. Statistical significance was calculated using Student's t-test for two-group comparisons and one-way or two-way ANOVA for multiple group comparisons (Prism; GraphPad, San Diego, CA).  $P < 5\%$  was considered statistically significant.

## RESULTS

### Static Mechanical Stress Increases the Levels of LC3-II in TM Cells

Primary cultures of human TM cells were grown to confluency and subjected to static sustained stretch of 20% elongation for up to 16 hours. The levels of the autophagosome marker LC3-II were evaluated by WB at the indicated times. As shown in Figures 1A and 1B, exposure to static mechanical stress caused an increase in the protein levels of LC3-II in TM cells compared to non-stretched cultures ( $p=0.0007$ , ANOVA,  $n=3$ ). This elevation in LC3-II could be observed as early as 30 min post-stretch ( $1.389 \pm 0.32$  fold,  $p>0.05$ ), reaching statistical significance at one hour post-stretch ( $1.56 \pm 0.05$ ,  $p<0.001$ ), and maintained throughout the duration of the experiment ( $1.909 \pm 0.054$ ;  $p<0.01$ ). To discern whether the observed increased LC3-II protein levels in the stretched cultures resulted from induction of autophagy versus decreased autophagic flux [30], cells were treated with the lysosomal basifying agent, CQ (30 nM), during the last hour of the stretching. Blockage of lysosomal degradation led to a further increase in LC3-II levels in CQ-treated cultures at one hour post-stretching compared to non-stretched ones, with no difference observed at later time points (Figure 1C). These results indicate that the elevation in LC3-II in the stretched cultures was, at least during the early times, mediated by the activation of the autophagy pathway in TM cells with mechanical stress. Partial lysosomal blockage with prolonged sustained stretch cannot, however, be excluded. To further confirm activation of autophagy, we treated the cultures with the autophagosome formation inhibitor 3-MA (10 mM), added to the culture media one hour prior to mechanical stress application (static, 20% elongation for 1 hour). As observed in Figure 2A, and quantified in Figure 2B, 3-MA significantly blocked the increase in LC3-II with mechanical stress ( $0.467 \pm 0.104$  RPL versus  $1.324 \pm 0.373$  RPL,  $p=0.0044$ ,  $n=4$ ).

We also examined by Western-blot the protein levels of other genes participating in the induction of autophagy or autophagic flux in mechanically stretched TM cells. We did not detect any significant variation in the expression of any of the proteins analyzed at 30

minutes or one hour post-stretching. At 16 hours, a significant decrease in the protein levels of Atg5, Atg7, and Atg12 was observed (Figure 3).

### Mechanical Stress Increases the Number and Size of Autolysosomes

To monitor autophagic flux we used the tFLC3 method [31]. This method relies on the different sensitivity to the acidic and/or proteolytic conditions of the lysosome lumen between GFP and RFP. The GFP fluorescence signal is sensitive, whereas mRFP is more stable. Therefore, colocalization of both GFP and RFP fluorescence highlights autophagosomes, which are yet not fused with lysosomes, whereas an mRFP signal without GFP corresponds to an autolysosome. Porcine TM cells infected with the recombinant adenovirus AdtFLC3 (m.o.i = 10 pfu/cell) [29] for two days were subjected to mechanical stress (20% elongation, 1 hour). As observed in Figure 4A, cells showed some degree of basal autophagy as demonstrated by the yellow/red puncta staining. Counting of yellow puncta per cell revealed a significant decrease in the number of autophagosomes in the stretched cells compared to non-stretched ( $11.13 \pm 12.30$  vs.  $37.00 \pm 38.34$  yellow puncta/cell,  $p=0.0007$ ,  $n=30$ ) (Figure 4B). In contrast, mechanically stressed cells displayed significantly higher amount of autolysosomes (red puncta,  $215.88 \pm 109.74$  vs.  $96.25 \pm 77.17$ ,  $p=0.0001$ ,  $n=30$ ). The red puncta/yellow puncta ratio was also higher in the stretched cells ( $38.15 \pm 35.93$ ,  $p=0.0001$ ,  $n=30$ ), which suggest that autophagic flux is not impaired, but that autophagosomes properly mature into autolysosomes (Figure 4C). Size measurements of the red and yellow puncta indicated larger size in both, autophagosomes ( $15.01 \pm 5.24$  vs.  $12.03 \pm 3.45$ ,  $p=0.0118$ ,  $n=30$ ) and autolysosomes ( $16.84 \pm 4.20$  vs.  $13.44 \pm 4.19$ ,  $p=0.0027$ ,  $n=30$ ) with mechanical stress (Figure 4D). Individual channels are included as Supplemental Material (SM-1).

We additionally examined the cellular ultrastructure by electron microscopy. Electron micrographs showed the existence of autophagic structures typified as membrane-bound organelles of ~ 500 nm in size in the cytosol of stretched cells (Figure 5B, representative examples are marked as asterisks), which could not been found in the control cells (Figure 5A). Higher magnification pictures demonstrated these organelles to be initial vacuoles or autophagosomes characterized by a double-membrane engulfing cytosolic-like material (Figure 5C, AVi), as well as degradative vacuoles (AVd), characterized by a single membrane containing amorphous electron-dense material and membranous structures (Figure 5C, AVd).

### Induction of Autophagy by Mechanical Stress is MTOR-Independent

Inhibition of the mechanistic target of rapamycin (MTOR) is the best-characterized signaling pathway known to activate autophagy, in particular in response to starvation, and in TM cells under chronic oxidative stress [29]. We investigated the potential role of MTOR pathway in stretched-induced autophagy by evaluating the phosphorylated levels of p70S6 Kinase (RPS6KB/p70S6K), a downstream target of MTOR, in porcine TM cells subjected to mechanical stress (20% elongation) for 1 hour. Porcine TM cells treated for 24 hours with rapamycin (1 $\mu$ M), an MTOR-dependent activator of autophagy, was included as a positive control. As observed in Figure 6A and quantified in Figure 6B, mechanically stressed TM cells showed higher relative protein levels of pRPS6KB ( $1.52 \pm 0.13$  vs.  $0.89 \pm$

0.14,  $p=0.009$ ,  $n=3$ ) compared to non-stretched ones, which evidence activation, rather than inhibition, of MTOR pathway. These results indicate that induction of autophagy with mechanical stress is MTOR-independent.

### Chaperon-Assisted Autophagy Does Not Mediate the Increase in LC3-II Levels in TM Cells Under Static Mechanical Stress

During the preparation of this manuscript, Ulbricht et al. reported a novel type of selective autophagy, chaperone-assisted autophagy (CASA), as a tension-induced autophagy pathway essential for mechanotransduction in mammalian cells [32]. In this model, the CASA complex senses the mechanical unfolding of filamin and initiates an ubiquitin-dependent autophagic sorting of damaged filamin to lysosomes for degradation. Since our results suggested the existence of an alternative pathway to MTOR pathway mediating the stretch-induced autophagy in our cultures, we decided to look at CASA. First, we checked whether filamin was being degraded through the lysosomal pathway in response to mechanical injury. For this, human TM cells were stretched in the presence of BafA1, a lysosomal inhibitor, or cycloheximide, a protein biosynthesis inhibitor. As shown in Figure 7A, none of the treatments caused any differences in the filamin protein levels in stretched cells compared to non-stretched ones, suggesting that CASA was not being activating in our experimental model. To further confirmed these results, we knocked down the expression of the co-chaperone BAG3, which is essential for CASA function, in the immortalized TM cell line (NTM), *via* siRNA (siBAG3). NTM transfected with a scrambled siRNA (siNC) or non-transfected cells were used as control. At day 2 post-transfection, cells were subjected to mechanical stress (20% elongation) for 16 hours. Similar to that observed in primary cultures, mechanically stressed NTM cells showed increased levels of LC3-II compared to non-stretched ones. Downregulation of BAG3 did not cause any differential expression in LC3-I, nor did it affect the increase in LC3-II with mechanical stress (Figure 7B). Likewise, we did not observe significant changes in the protein levels of filamin in the cells transfected with siBAG3 or in the stretched cultures (Figure 7A and B).

### Induction of Autophagy in High Pressure-Perfused Eyes

The experiments presented so far have been conducted in an *in vitro* cell culture model, which mimics the deformations that TM cells experience *in vivo* with ocular hypertension. We wanted to examine whether stretching of TM cells *in situ* as a result of elevated IOP also activates autophagy. For this, enucleated porcine eyes were perfused for one hour at either normal physiological pressure (8 mmHg equivalent to 15 mmHg *in vivo*), or at high pressure (fellow eye, 30 mmHg). As seen in Figure 8A, perfusion of eyes at 30 mmHg resulted in increased levels of LC3-II compared to those ones perfused at 8 mmHg (Figure 8B,  $4.311 \pm 0.249$  vs  $2.620 \pm 0.278$ ,  $p=0.0001$ ,  $n=6$ ). Ultrastructural analysis also demonstrated the presence of autophagosomes and autolysosomes figures in the cells of the corneoscleral meshwork of eyes perfused at high pressure, which were not observed in control eyes (Figure 8C, arrowheads).

## DISCUSSION

Cells in the TM are constantly subjected to mechanical strain associated with elevations in IOP. In order to preserve cellular function and regain homeostasis, cells must adapt to these morphological changes. Here, we have shown the induction of autophagy, a survival adaptive pathway, in TM cells in response to static biaxial stretch as well as in high-pressure perfused eyes. We further showed that the induction of autophagy with mechanical stretch in TM cells is MTOR- and BAG3 independent. To our knowledge this is the first study reporting the induction of autophagy with mechanical strain.

Static biaxial strain was chosen for our *in vitro* experimental model to mimic acute sustained elevation of IOP, similar to that occurring under ocular hypertension and glaucoma. Although no studies have looked at the level of strain experienced by TM cells for a given degree of pressure elevation, the 20% elongation used in our experiments falls within the pathophysiological ranges [33,34]. Under these conditions, we observed a dramatic increase in the levels of the autophagosome marker LC3-II in the mechanically stretched cultures. Inhibition of lysosomal degradation with CQ further increased the amount of LC3-II at early times post-stretching, while pharmacological blockage of autophagosome formation with 3-MA prevented it. Altogether, our data indicate that the stretch-induced increase in LC3-II results from induction of autophagy, and it is mediated by the development of new autophagosomes. Should we note that no changes in the quantity of p62/SQSTM1, an ubiquitin receptor that links ubiquitinated proteins to the autophagy machinery, were observed with mechanical strain [35]. Although p62 protein levels have been used as a readout for autophagic degradation, as recently indicated in [30], there is not always a clear correlation between increases in LC3-II and decreases in SQSTM1. A potential explanation for that, among others, is simultaneous transcriptional induction of the gene encoding for p62.

The quick activation of autophagy, as early as 30 minutes post-stretch, reasonably supports a role of the autophagic pathway as one of the initial responses elicited in TM cells to cope with the stress exerted by mechanical forces. Still higher LC3-II levels were found in the stretched cultures after 16 hours of static stretch. A priori, one would expect cells subjected to static mechanical stretch to adapt to their new environment by for example adjusting their attachment to the substratum and thereby reducing the mechanical strain, or by changes in the cytoskeleton. In a recent study, induction of autophagy was observed in both *Dictyostelium* and a breast cancer cell line when subjected to mechanical compressive stress [36]. In this case, induction of autophagy was transient and LC3-II reverted to its basal levels after 90 minutes, when cells recovered their shape. It is unclear how long it takes stretched TM cells to adapt to mechanical forces. Although the higher LC3-II levels after 16 hours of constant stretch could indicate that the strain-induced stress was still not completely relieved, we also observed at this specific time-point a decrease in the amount of Atg5 and Atg12 in the stretched cultures. The Atg5-Atg12 conjugate is essential for LC3 lipidation and subsequent autophagosome formation. Interestingly, downregulation of Atg5-Atg12 has been shown to be a key event in controlling basal autophagy [37]. It is therefore plausible that a regulatory negative feedback has been already initiated in these cells. This is



in accordance with the reported regain of the normal morphological appearance in TM cells within 24 hours of static stretching [8].

It should also be considered such increase in LC3-II levels to result from concomitant impaired or delayed autophagic flux under prolonged strain, specially since no significant changes in LC3-II were detected among non-stretched and stretched cultures in the presence of CQ at longer times [38]. In order for autophagy to be successful, autophagosomes must fuse with lysosomes, so that cargo material can be degraded within autolysosomes. For this, once they have formed, autophagosomes travel bi-directionally along microtubules towards lysosomes, which are concentrated around the centrosome in the perinuclear region [39]. Microtubules are structural components of the cytoskeleton that determine cell shape, polarity, and motility in cooperation with the actin filaments. Mechanical stretch is known to disrupt cytoskeleton, including microtubules [40,41]. Therefore, it was plausible that disruption of the microtubular network with mechanical stretch could mislocate autophagosomes and lysosomes. The pattern of staining obtained when evaluating autophagic dynamics using the tFLC3 assay showed a functional autophagic maturation process in the stretched cultures, with a significant increase of red-only puncta [24]. Moreover, our data indicated that not only mechanical stretch does not perturb maturation of autophagosomes into autolysosomes but also that the number and size of autolysosomes was higher in mechanically stretched cells. Electron microscopy analysis qualitatively confirmed the presence of autophagic structures (initial and degradative vacuoles) in cell subjected to mechanical strain.

It is important to emphasize that the decrease in autophagosome number observed in the stretched cultures is not inconsistent with induction of autophagy, as determined by LC3 lipidation. In contrast to the LC3-II WB, the tFLC3 assay does not evaluate autophagosome formation, but autophagic dynamics. Autophagosomes are highly dynamic structures that rapidly fuse with lysosomes, as early as 5 min after formation [42], unless fusion between autophagosomes and lysosomes is blocked, for example with vinblastine. We could not perform this type of experiments since the drug would affect the stretch response. Another factor to consider is that that LC3 WB also detects LC3-II located in the phagophore (or isolation membrane) and incomplete autophagosomes.

The signaling pathway triggering induction of autophagy with mechanical stretch has still to be identified. In agreement with previous reports [12], static stretch activates MTOR pathway, the classical autophagy inhibitor pathway, in TM cells. MTOR-independent activation of autophagy has also been reported in breast cancer cells subjected to mechanical compression [36]. This and our study suggest the existence of an alternative mechanosensitive activator of autophagy that override the inhibitory signals triggered from stretch-induced MTOR activation. One potential option to this alternative pathway is CASA, a tension-induced autophagy pathway essential for mechanotransduction that has been very recently described in mammalian cells [32]. In this model, the CASA complex senses the mechanical unfolding of filamin and initiates an ubiquitin-dependent autophagic sorting of damaged filamin to lysosomes for degradation. We did not detect, however, changes in the filamin or the chaperon BAG3 protein levels with mechanical stress, even in the presence of BafA1 or Chx. Furthermore, increased LC3-II was still observed in siBAG3-transfected

cells in response to stretch. Therefore, the induction of autophagy with mechanical stress does not seem to be mediated by CASA in our system. However, we do not rule out CASA to be activated in other experimental conditions that might more extensively damage cytoskeleton components.

Our experiments here have confirmed the occurrence of autophagy in high pressure perfused eyes compared to eyes perfused at normal pressure conditions, characterized by elevated LC3-II levels and the presence of autophagic figures in the cells of the corneoscleral meshwork. Earlier studies by Grierson et al. also described increased size and number of lysosomes and lysosomal complexes in the outflow pathway cells of Rhesus monkeys subjected to high IOP [2]. Two immediate questions arise from these studies: (1) whether autophagy is a primary response to elevated pressure (act as a mechanosensor) or it is a secondary response to morphological tissue deformations, similar to those described by Battista et al. [43]; and (2) which is the role of stretch-induced autophagy in cellular and tissue physiology.

Although a limited number of studies in the literature have reported activation of autophagy with mechanical compression and fluid shear stress [36,44–46], the physiological or pathophysiological implications of mechanically-induced autophagy are not known at present. One potential role is adaptation [47]. When subjected to forces or elevated pressure, TM cells must modify and reinforce their cytoskeleton to increase cortical rigidity. Induction of autophagy can help cells to undergo these changes by increasing protein and organelle turnover, which might in turn affect other cellular and metabolic processes to help rebalance cellular and tissue function. The experimental conditions used in this study (30 mmHg, 1 hour) were aimed at addressing whether induction of autophagy was an early response to short-term acute elevation in IOP. Unfortunately, we could not perform any physiological study by using this experimental model. However, long-term perfusion experiments conducted in different laboratories, have suggested the existence of some compensatory pressure-lowering mechanism in the trabecular outflow pathway in response to more physiologic pressure elevations [11,48]. Whether the initial activation of autophagy forms part of this compensatory homeostatic mechanism by facilitating secondary adaptation, such as ECM remodeling or mechanical signaling to stretch [34], is an exciting possibility that needs to be further explored.

Another potential role of autophagy might be that of protecting against stretched-induced injury and determining cell fate. Although autophagy is generally regarded as a prosurvival mechanism, a number of studies indicate a complex relationship between autophagy and apoptosis. Induction of autophagy promotes survival through inhibition of apoptosis *via* direct interaction between Beclin 1 and Bcl 2 [49]. However, continuous activation of autophagy can also lead to autophagic cell death [50,51]. Thus, mechanical activation of autophagy under normal physiological forces may help remove damaged components and suppress cell death. In this sense, a recent study has shown rapamycin, an autophagy activator, to efficiently protect against the damaging effects of compressive mechanical stress and biochemical stimuli in articular cartilage [52]. In contrast, if mechanical forces exceed the physiological ranges or under pathological conditions, dysregulation of autophagy might trigger cell death and contribute to disease [44,45]. The stretching

conditions used in these experiments did not elicit cell death. Some degree of cytotoxicity was observed when using 3-MA (data not shown), which might point out towards a pro-survival role of autophagy in TM cells against mechanical strain. We are currently working towards developing molecular tools to better address this question.

## CONCLUSIONS

In summary, our data here shows for the first time the activation of autophagy under biaxial mechanical stretch and high pressure in TM cells in an MTOR- and BAG3 independent manner. We hypothesize that activation of autophagy is part of the physiological response to maintain TM cellular homeostasis and adaptation to mechanical forces. Future studies will be directed at elucidating the precise role and the signaling pathways participating in the stretch-induced autophagy, and its potential role in outflow pathway pathophysiology in ocular hypertension and glaucoma. Whether autophagy is impaired in glaucoma is currently under investigation.

## Supplementary Material

Refer to Web version on PubMed Central for supplementary material.

## Acknowledgments

The authors would like to thank Ying Hao for excellent technical assistance in the TEM. This work was supported by National Institute of Health Grants R01EY020491 (Liton) and P30EY005722; the Brightfocus Foundation (Liton, G2012022), the Alcon Foundation (Liton, Young Investigator Grant), and by an unrestricted grant to Duke Eye Center from Research to Prevent Blindness.

## ABBREVIATIONS

<b>TM</b>	trabecular meshwork
<b>IOP</b>	intraocular pressure
<b>ATG</b>	autophagy-related genes
<b>CTSB</b>	cathepsin B
<b>BECN1</b>	beclin
<b>TUBB</b>	beta tubulin
<b>SQSTM</b>	sequestosome
<b>tfLC3</b>	tandem fluorescence LC3
<b>GFP</b>	green fluorescence protein
<b>RFP</b>	red fluorescence protein
<b>m.o.i</b>	multiplicity of infection
<b>BafA1</b>	bafilomycin A1
<b>MTOR</b>	mammalian target of rapamycin

<b>3-MA</b>	3-methyladenine
<b>Chx</b>	cycloheximide
<b>CQ</b>	chloroquine
<b>CASA</b>	chaperon-assisted autophagy
<b>FLNA</b>	filamin A
<b>BAG3</b>	Bcl-2-associated athanogene 3

## REFERENCES

- [1]. Stamer WD, Acott TS. Current understanding of conventional outflow dysfunction in glaucoma. *Curr Opin Ophthalmol.* 2012; 23:135–143. [PubMed: 22262082]
- [2]. Grierson I, Lee WR. The fine structure of the trabecular meshwork at graded levels of intraocular pressure. (1) Pressure effects within the near-physiological range (8–30 mmHg). *Exp Eye Res.* 1975; 20:505–521. [PubMed: 1149832]
- [3]. Johnstone MA, Grant WG. Pressure-dependent changes in structures of the aqueous outflow system of human and monkey eyes. *Am J Ophthalmol.* 1973; 75:365–383. [PubMed: 4633234]
- [4]. Coleman DJ, Trokel S. Direct-recorded intraocular pressure variations in a human subject. *Arch Ophthalmol.* 1969; 82:637–640. [PubMed: 5357713]
- [5]. Matsuo T, Uchida H, Matsuo N. Bovine and porcine trabecular cells produce prostaglandin F<sub>2</sub> alpha in response to cyclic mechanical stretching. *Jpn J Ophthalmol.* 1996; 40:289–296. [PubMed: 8988417]
- [6]. Mitton KP, Tumminia SJ, Arora J, Zelenka P, Epstein DL, Russell P. Transient loss of alphaB-crystallin: an early cellular response to mechanical stretch. *Biochem Biophys Res Commun.* 1997; 235:69–73. [PubMed: 9196037]
- [7]. Okada Y, Matsuo T, Ohtsuki H. Bovine trabecular cells produce TIMP-1 and MMP-2 in response to mechanical stretching. *Jpn J Ophthalmol.* 1998; 42:90–94. [PubMed: 9587839]
- [8]. Tumminia SJ, Mitton KP, Arora J, Zelenka P, Epstein DL, Russell P. Mechanical stretch alters the actin cytoskeletal network and signal transduction in human trabecular meshwork cells. *Invest Ophthalmol Vis Sci.* 1998; 39:1361–1371. [PubMed: 9660484]
- [9]. Sato Y, Matsuo T, Ohtsuki H. A novel gene (oculomedin) induced by mechanical stretching in human trabecular cells of the eye. *Biochem Biophys Res Commun.* 1999; 259:349–351. [PubMed: 10362512]
- [10]. WuDunn D. The effect of mechanical strain on matrix metalloproteinase production by bovine trabecular meshwork cells. *Curr Eye Res.* 2001; 22:394–397. [PubMed: 11600941]
- [11]. Bradley JM, Kelley MJ, Zhu X, Anderssohn AM, Alexander JP, Acott TS. Effects of mechanical stretching on trabecular matrix metalloproteinases. *Invest Ophthalmol Vis Sci.* 2001; 42:1505–1513. [PubMed: 11381054]
- [12]. Bradley JMB, Kelley MJ, Rose A, Acott TS. Signaling pathways used in trabecular matrix metalloproteinase response to mechanical stretch. *Invest Ophthalmol Vis Sci.* 2003; 44:5174–5181. [PubMed: 14638714]
- [13]. Vittal V, Rose A, Gregory KE, Kelley MJ, Acott TS. Changes in gene expression by trabecular meshwork cells in response to mechanical stretching. *Invest Ophthalmol Vis Sci.* 2005; 46:2857–2868. [PubMed: 16043860]
- [14]. Liton PB, Liu X, Challa P, Epstein DL, Gonzalez P. Induction of TGF-beta1 in the trabecular meshwork under cyclic mechanical stress. *J Cell Physiol.* 2005; 205:364–371. [PubMed: 15895394]
- [15]. Liton PB, Luna C, Bodman M, Hong A, Epstein DL, Gonzalez P. Induction of IL-6 expression by mechanical stress in the trabecular meshwork. *Biochem Biophys Res Commun.* 2005; 337:1229–1236. [PubMed: 16229816]

- [16]. Chudgar SM, Deng P, Maddala R, Epstein DL, Rao PV. Regulation of connective tissue growth factor expression in the aqueous humor outflow pathway. *Mol Vis.* 2006; 12:1117–1126. [PubMed: 17093396]
- [17]. Keller KE, Kelley MJ, Acott TS. Extracellular matrix gene alternative splicing by trabecular meshwork cells in response to mechanical stretching. *Invest Ophthalmol Vis Sci.* 2007; 48:1164–1172. [PubMed: 17325160]
- [18]. Luna C, Li G, Liton PB, Epstein DL, Gonzalez P. Alterations in gene expression induced by cyclic mechanical stress in trabecular meshwork cells. *Mol Vis.* 2009; 15:534–544. [PubMed: 19279691]
- [19]. Luna C, Li G, Qiu J, Challa P, Epstein DL, Gonzalez P. Extracellular release of ATP mediated by cyclic mechanical stress leads to mobilization of AA in trabecular meshwork cells. *Invest Ophthalmol Vis Sci.* 2009; 50:5805–5810. [PubMed: 19608543]
- [20]. Boya P, Reggiori F, Codogno P. Emerging regulation and functions of autophagy. *Nat Cell Biol.* 2013; 15:713–720. [PubMed: 23817233]
- [21]. Mizushima N. Autophagy: process and function. *Genes Dev.* 2007; 21:2861–2873. [PubMed: 18006683]
- [22]. Kabeya Y, Mizushima N, Ueno T, Yamamoto A, Kirisako T, Noda T, et al. LC3, a mammalian homologue of yeast Apg8p, is localized in autophagosome membranes after processing. *Embo J.* 2000; 19:5720–5728. [PubMed: 11060023]
- [23]. Kuma A, Matsui M, Mizushima N. LC3, an autophagosome marker, can be incorporated into protein aggregates independent of autophagy: caution in the interpretation of LC3 localization. *Autophagy.* 2007; 3:323–328. [PubMed: 17387262]
- [24]. Kimura S, Fujita N, Noda T, Yoshimori T. Monitoring autophagy in mammalian cultured cells through the dynamics of LC3. *Meth Enzymol.* 2009; 452:1–12. [PubMed: 19200872]
- [25]. Martina JA, Chen Y, Gucek M, Puertollano R. MTORC1 functions as a transcriptional regulator of autophagy by preventing nuclear transport of TFEB. *Autophagy.* 2012; 8:903–914. [PubMed: 22576015]
- [26]. Pattingre S, Espert L, Biard-Piechaczyk M, Codogno P. Regulation of macroautophagy by mTOR and Beclin 1 complexes. *Biochimie.* 2008; 90:313–323. [PubMed: 17928127]
- [27]. Liton PB, Lin Y, Luna C, Li G, Gonzalez P, Epstein DL. Cultured porcine trabecular meshwork cells display altered lysosomal function when subjected to chronic oxidative stress. *Invest Ophthalmol Vis Sci.* 2008; 49:3961–3969. [PubMed: 18469195]
- [28]. Pang IH, Shade DL, Clark AF, Steely HT, DeSantis L. Preliminary characterization of a transformed cell strain derived from human trabecular meshwork. *Curr Eye Res.* 1994; 13:51–63. [PubMed: 8156826]
- [29]. Porter K, Nallathambi J, Lin Y, Liton PB. Lysosomal basification and decreased autophagic flux in oxidatively stressed trabecular meshwork cells: implications for glaucoma pathogenesis. *Autophagy.* 2013; 9:581–594. [PubMed: 23360789]
- [30]. Klionsky DJ, Abdalla FC, Abeliovich H, Abraham RT, Acevedo-Arozena A, Adeli K, et al. Guidelines for the use and interpretation of assays for monitoring autophagy. *Autophagy.* 2012; 8:445–544. [PubMed: 22966490]
- [31]. Kimura S, Noda T, Yoshimori T. Dissection of the autophagosome maturation process by a novel reporter protein, tandem fluorescent-tagged LC3. *Autophagy.* 2007; 3:452–460. [PubMed: 17534139]
- [32]. Ulbricht A, Eppler FJ, Tapia VE, van der Ven PFM, Hampe N, Hersch N, et al. Cellular Mechanotransduction Relies on Tension-Induced and Chaperone-Assisted Autophagy. *Curr Biol.* 2013
- [33]. WuDunn D. Mechanobiology of trabecular meshwork cells. *Exp Eye Res.* 2009; 88:718–723. [PubMed: 19071113]
- [34]. Acott TS, Kelley MJ, Keller KE, Vranka JA, Abu-Hassan DW, Li X, et al. Intraocular Pressure Homeostasis: Maintaining Balance in a High-Pressure Environment. *J Ocul Pharmacol Ther.* 2014

- [35]. Pankiv S, Clausen TH, Lamark T, Brech A, Bruun J-A, Outzen H, et al. p62/SQSTM1 binds directly to Atg8/LC3 to facilitate degradation of ubiquitinated protein aggregates by autophagy. *J Biol Chem*. 2007; 282:24131–24145. [PubMed: 17580304]
- [36]. King JS, Veltman DM, Insall RH. The induction of autophagy by mechanical stress. *Autophagy*. 2011; 7:1490–1499. [PubMed: 22024750]
- [37]. Xia H-G, Zhang L, Chen G, Zhang T, Liu J, Jin M, et al. Control of basal autophagy by calpain1 mediated cleavage of ATG5. *Autophagy*. 2010; 6:61–66. [PubMed: 19901552]
- [38]. Mizushima N, Yoshimori T. How to interpret LC3 immunoblotting. *Autophagy*. 2007; 3:542–545. [PubMed: 17611390]
- [39]. Kimura S, Noda T, Yoshimori T. Dynein-dependent movement of autophagosomes mediates efficient encounters with lysosomes. *Cell Struct Funct*. 2008; 33:109–122. [PubMed: 18388399]
- [40]. Celik E, Abdulreda MH, Maiguel D, Li J, Moy VT. Rearrangement of microtubule network under biochemical and mechanical stimulations. *Methods*. 2013; 60:195–201. [PubMed: 23466787]
- [41]. Gautel M. Cytoskeletal protein kinases: titin and its relations in mechanosensing. *Pflugers Arch*. 2011; 462:119–134. [PubMed: 21416260]
- [42]. Lawrence BP, Brown WJ. Autophagic vacuoles rapidly fuse with pre-existing lysosomes in cultured hepatocytes. *J Cell Sci*. 1992; 102(Pt 3):515–526. [PubMed: 1324248]
- [43]. Battista SA, Lu Z, Hofmann S, Freddo T, Overby DR, Gong H. Reduction of the available area for aqueous humor outflow and increase in meshwork herniations into collector channels following acute IOP elevation in bovine eyes. *Invest Ophthalmol Vis Sci*. 2008; 49:5346–5352. [PubMed: 18515571]
- [44]. Tanabe F, Yone K, Kawabata N, Sakakima H, Matsuda F, Ishidou Y, et al. Accumulation of p62 in degenerated spinal cord under chronic mechanical compression: functional analysis of p62 and autophagy in hypoxic neuronal cells. *Autophagy*. 2011; 7:1462–1471. [PubMed: 22082874]
- [45]. Ma K-G, Shao Z-W, Yang S-H, Wang J, Wang B-C, Xiong L-M, et al. Autophagy is activated in compression-induced cell degeneration and is mediated by reactive oxygen species in nucleus pulposus cells exposed to compression. *Osteoarthritis Cartil*. 2013
- [46]. Lien S-C, Chang S-F, Lee P-L, Wei S-Y, Chang MD-T, Chang J-Y, et al. Mechanical regulation of cancer cell apoptosis and autophagy: Roles of bone morphogenetic protein receptor, Smad1/5, and p38 MAPK. *Biochim Biophys Acta*. 2013; 1833:3124–3133. [PubMed: 24021264]
- [47]. King JS. Mechanical stress meets autophagy: potential implications for physiology and pathology. *Trends in Molecular Medicine*. 2012; 18:583–588. [PubMed: 22981844]
- [48]. Borrás T, Rowlette LLS, Tamm ER, Gottanka J, Epstein DL. Effects of elevated intraocular pressure on outflow facility and TIGR/MYOC expression in perfused human anterior segments. *Invest Ophthalmol Vis Sci*. 2002; 43:33–40. [PubMed: 11773009]
- [49]. Levine B, Sinha S, Kroemer G. Bcl-2 family members: dual regulators of apoptosis and autophagy. *Autophagy*. 2008; 4:600–606. [PubMed: 18497563]
- [50]. Kroemer G, Levine B. Autophagic cell death: the story of a misnomer. *Nat Rev Mol Cell Biol*. 2008; 9:1004–1010. [PubMed: 18971948]
- [51]. Lenardo MJ, McPhee CK, Yu L. Autophagic cell death. *Meth Enzymol*. 2009; 453:17–31. [PubMed: 19216900]
- [52]. Caramés B, Taniguchi N, Seino D, Blanco FJ, D'Lima D, Lotz M. Mechanical injury suppresses autophagy regulators and pharmacologic activation of autophagy results in chondroprotection. *Arthritis Rheum*. 2012; 64:1182–1192. [PubMed: 22034068]

**HIGHLIGHTS**

- Static mechanical stretch induces autophagy in TM cells
- Autophagy is induced in TM cells in high-pressure perfused eyes
- Stretch-induced autophagy in TM cells is MTOR-independent
- CASA does not mediate the induction of autophagy in TM cells under static stretch

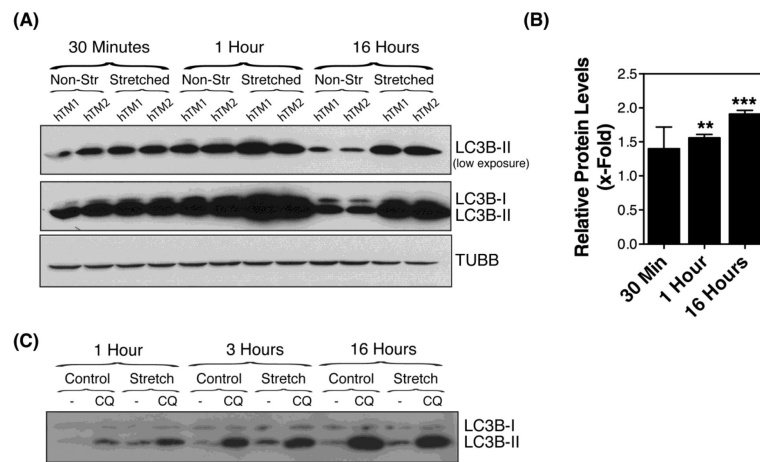


**Figure 1.**

LC3-I to LC3-II turnover in human TM cells subjected to static mechanical stress. (A) Protein expression levels of LC3-I and LC3-II in primary cultures of human TM cells subjected to static mechanical stress (20% elongation) for 30 min, 1 hour or 16 hours, evaluated by WB analysis. TUBB/ $\beta$ -tubulin was used as loading control. (B) Normalized fold-changes of LC3B-II in stretched cultures compared to non-stretched cultures calculated from densitometric analysis of the blots. (C) Expression levels of LC3-I and LC3-II in TM cells mechanically stressed (static, 20% elongation) treated with CQ (30 nM), added during the last hour of the stretching. Data are mean  $\pm$  SD,  $n=3$ , \*\* $p < 0.001$ , \*\*\*  $p < 0.0001$ , one-way ANOVA with Bonferroni post hoc test.



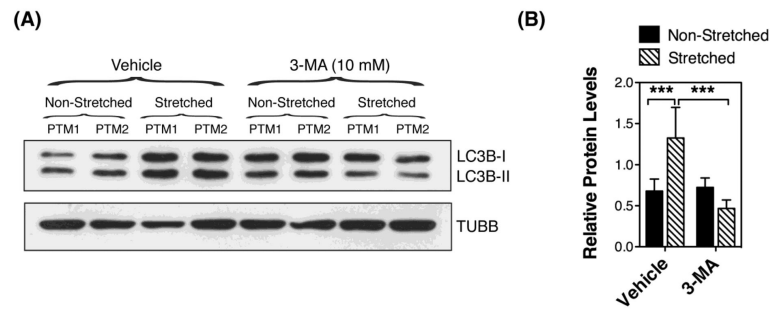


**Figure 2.**

Autophagy inhibition in mechanically stressed TM cells. (A) Protein expression levels of LC3-I and LC3-II in TM cells subjected to static mechanical stress (20% elongation, 1hour) in the presence of 3-MA (10 mM) added to the culture media one hour prior to stretching, evaluated by WB analysis. TUBB was used as loading control. Blots are representative from four independent experiments. (B) Normalized relative protein levels of LC3B-II calculated from densitometric analysis of the blots. Data are the means  $\pm$  SD,  $n = 4$ ,  $***p < 0.001$ , t-test.

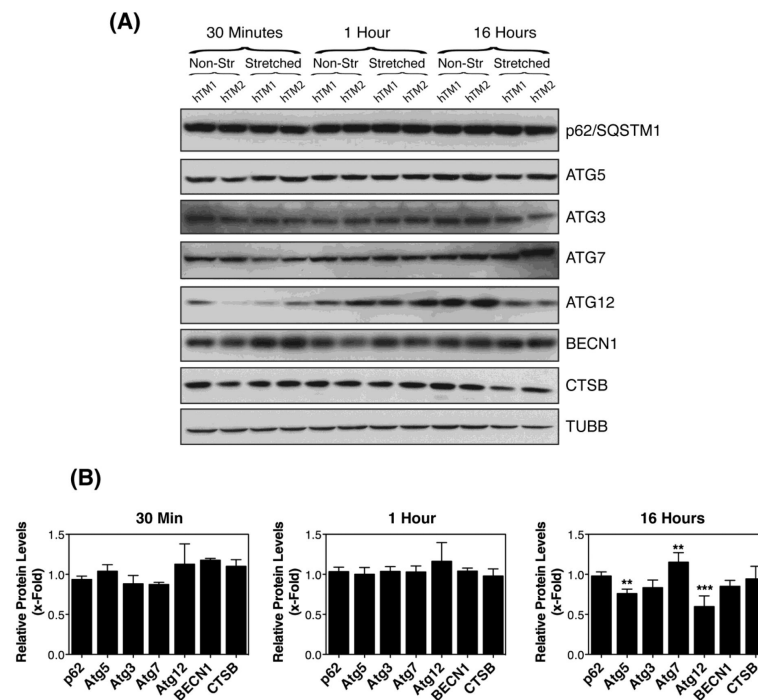


**Figure 3.** Expression levels of proteins participating in the induction of autophagy or autophagic flux in mechanically stretched TM cells. (A) Representative immunoblots using the indicated specific antibodies. (B) Normalized relative protein levels calculated from densitometric analysis of the blots. Data are the means  $\pm$  SD,  $n = 4$ , \* $p < 0.05$ , \*\* $p < 0.001$ , Two-way ANOVA followed by Bonferroni's post hoc test.

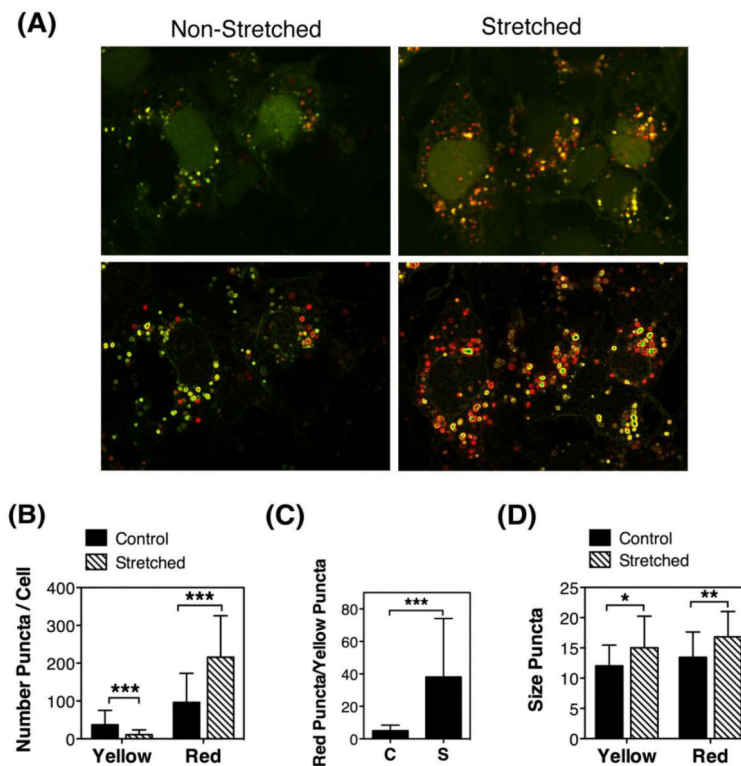


**Figure 4.** Autophagic flux in mechanically stressed TM cells evaluated by tfLC3: Primary cultures of TM cells were infected with AdtfLC3 (m.o.i = 10 pfu/cell). At 2 d.p.i., cells were subjected to mechanical stress (20% elongation, 1 hour). (A) Representative confocal images showing the presence of yellow and red puncta in non-stretched and stretched cells. Bottom panels represents the top panel pictures processed with the Find Edges tools in Image J to facilitate manual counting. (B) Number of yellow and red puncta per cell. (C) Autophagic flux measurement as a ratio of red/yellow puncta per cell. (D) Size of yellow and red puncta. Data are means  $\pm$  SD of three independent experiments, ten cells/experiment,  $n = 30$ , \* $p < 0.05$ , \*\* $p < 0.00$ , \*\*\*  $p < 0.0001$ , t-test.

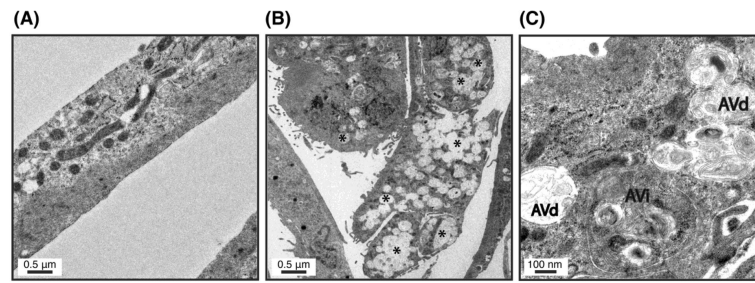


**Figure 5.**

Ultrastructural appearance of TM cells exposed to static mechanical stress. (A) Non-stretched cells. (B) Stretched cells. (C) Stretched cells at higher magnification. Note the intracellular presence of autophagic structures (B, representative examples marked as \*) in the cells subjected to mechanical stress identified as initial vacuoles (C, AVi) and degradative vacuoles (C, AVd). Pictures are representative of three independent experiments.

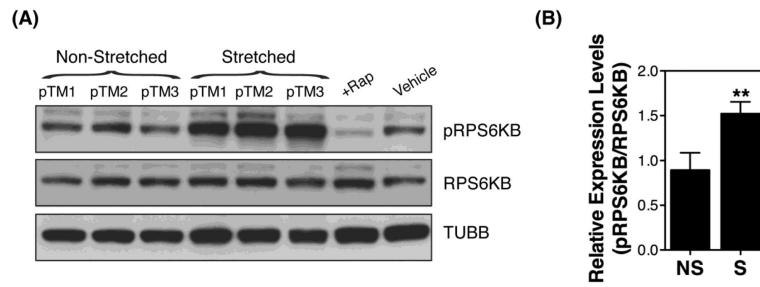


**Figure 6.** MTOR pathway in mechanically stressed TM cells. (A) Protein levels of phosphorylated and non-phosphorylated downstream target of MTOR, RPS6KB. (B) Normalized relative protein levels of pRPS6KB calculated from densitometric analysis of the blots. Data are the means  $\pm$  SD, n = 3, \*\*p < 0.01, t-test. NS: non-stretched; S: stretched.

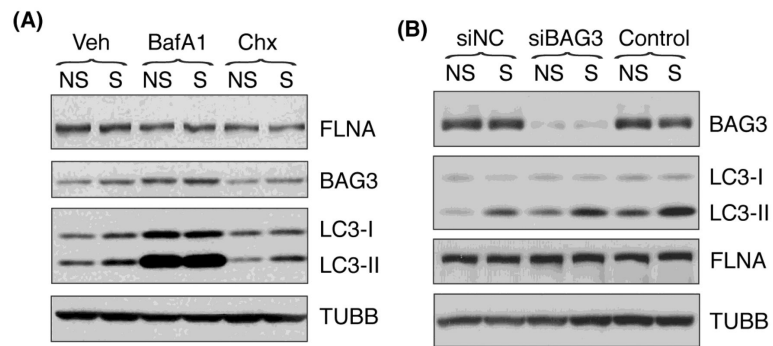


**Figure 7.**

Chaperon-assisted autophagy in TM cells under static mechanical stress: Protein levels of the CASA components FLNA and BAG3, as well as the autophagic marker LC3-II in (A) HTM cells subjected to static stretch (20% elongation, 16 hours) in the presence of BafA1 (100 nM) or Chx (25  $\mu$ M) added to the culture media 30 minutes prior to stretching; (B) NTM cells transfected with siBAG3. TUBB was used as loading control. Blots are representative from three independent experiments.

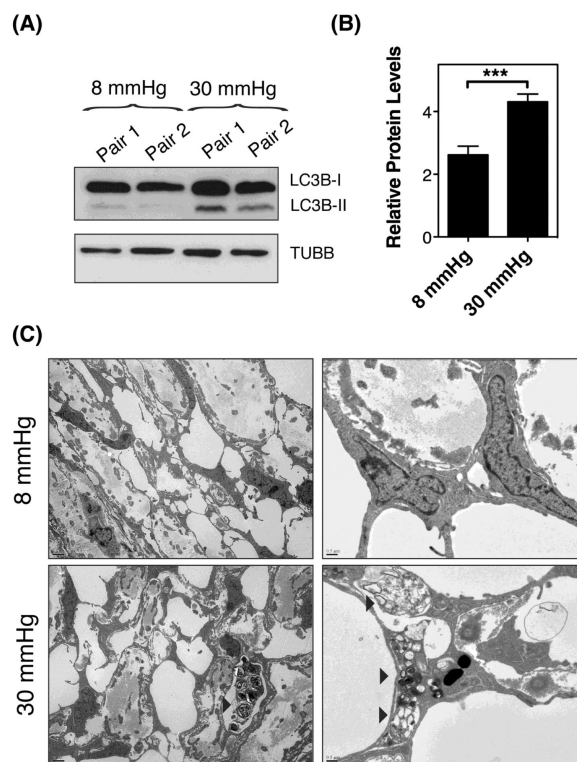


**Figure 8.** Induction of Autophagy in High Pressure-Perfused Eyes. Enucleated porcine eyes were perfused for one hour at either normal physiological pressure (8 mmHg equivalent to 15 mmHg *in vivo*), or at high pressure (fellow eye, 30 mmHg). (A) Protein expression levels of LC3-I and LC3-II. (B) Normalized relative protein levels of LC3B-II calculated from densitometric analysis of the blots. (C) Electron micrographs showing the presence of autophagic figures (arrowheads) in the cells of the corneoscleral meshwork of eyes perfused at high pressure.

**Table 1**

## List of Primary Antibodies Used

Target Protein	Company	Catalog Number	Dilution
LC3A/B	Abcam	ab58610	1:500
LC3B	Cell Signaling	3868S	1:1000
SQSTM1	Sigma-Aldrich	P0067	1:1000
TUBB	Sigma-Aldrich	T5893	1:1000
ATG5	Cell Signaling	8540P	1:1000
BECN1	Cell Signaling	3495P	1:1000
ATG7	Cell Signaling	2631P	1:1000
ATG12	Cell Signaling	4180P	1:1000
CTSB	Abcam	ab58802	1:1000
p70S6K	Santa Cruz Biotechnology	SC-230	1:1000
p-p70S6K	Santa Cruz Biotechnology	SC-7984-R	1:1000
BAG3	Millipore	ABC277	1:2000
FLNA	Millipore	MAB1672	1:2500